HHS Public Access

Author manuscript

Int J Radiat Oncol Biol Phys. Author manuscript; available in PMC 2016 March 01.

Published in final edited form as:

Int J Radiat Oncol Biol Phys. 2015 September 1; 93(1): 166–172. doi:10.1016/j.ijrobp.2015.05.016.

Indirect Tumor Cell Death After High-Dose Hypofractionated Irradiation: Implications for Stereotactic Body Radiation Therapy and Stereotactic Radiation Surgery

Chang W. Song, PhD[*,†], **Yoon-Jin Lee, PhD**[†], **Robert J. Griffin, PhD**[‡], **Inhwan Park, BA**[*], **Nathan A. Koonce, PhD**[‡], **Susanta Hui, PhD**[*], **Mi-Sook Kim, MD, PhD**[†], **Kathryn E. Dusenbery, MD**[*], **Paul W. Sperduto, MD**[§], and **L. Chinsoo Cho, MD**[*]

[*]Department of Therapeutic Radiology-Radiation Oncology, University of Minnesota Medical School, Minneapolis, Minnesota

[†]Korea Institute of Radiological and Medical Sciences, Seoul, Korea

[‡]Department of Radiation Oncology, University of Arkansas for Medical Sciences, Little Rock, Arkansas

[§]Minneapolis Radiation Oncology and Gamma Knife Center, University of Minnesota, Minneapolis, Minnesota

Summary

In experimental mouse tumors, high-dose irradiation in a single fraction caused progressive increase in tumor cell death in 2 to 5 days. Such delayed tumor cell deaths appeared to be due to radiation-induced deterioration of intratumor microenvironment characterized by profound reduction of blood perfusion and increase in hypoxia. Similar secondary and indirect cell death may play an important role in clinical stereotactic body radiation therapy and stereotactic radiation surgery.

Purpose—The purpose of this study was to reveal the biological mechanisms underlying stereotactic body radiation therapy (SBRT) and stereotactic radiation surgery (SRS).

Methods and Materials—FSaII fibrosarcomas grown subcutaneously in the hind limbs of C3H mice were irradiated with 10 to 30 Gy of X rays in a single fraction, and the clonogenic cell survival was determined with in vivo—in vitro excision assay immediately or 2 to 5 days after irradiation. The effects of radiation on the intratumor microenvironment were studied using immunohistochemical methods.

Results—After cells were irradiated with 15 or 20 Gy, cell survival in FSaII tumors declined for 2 to 3 days and began to recover thereafter in some but not all tumors. After irradiation with 30 Gy, cell survival declined continuously for 5 days. Cell survival in some tumors 5 days after 20 to 30 Gy irradiation was 2 to 3 logs less than that immediately after irradiation. Irradiation with 20 Gy markedly reduced blood perfusion, upregulated HIF-1α, and increased carbonic anhydrase-9 expression, indicating that irradiation increased tumor hypoxia. In addition, expression of VEGF

Reprint requests to: Chang W. Song, PhD, Department of Therapeutic Radiology-Radiation Oncology, University of Minnesota Medical School, Minneapolis, MN 55455. Tel: (612) 626-6852; songx001@umn.edu.

also increased in the tumor tissue after 20 Gy irradiation, probably due to the increase in HIF-1α activity.

Conclusions—Irradiation of FSaII tumors with 15 to 30 Gy in a single dose caused dose-dependent secondary cell death, most likely by causing vascular damage accompanied by deterioration of intratumor microenvironment. Such indirect tumor cell death may play a crucial role in the control of human tumors with SBRT and SRS.

Introduction

Recently, increasing numbers of cancer patients have been treated with stereotactic body radiation therapy (SBRT) or stereotactic radiation surgery (SRS). These technologies accurately deliver high-dose radiation in a single fraction or in 2 to 5 fractions to a target tumor volume, with acceptable radiation dose to normal tissues (1–5). Such a paradigm shift from conventional multifractionated radiation therapy to SBRT and SRS has been possible as a result of the remarkable improvement in tumor imaging and irradiation techniques. However, the biological mechanism underlying SBRT and SRS has been elusive (6–10).

It has been suggested that secondary, or indirect, cell death as a result of vascular damage plays an important role in tumors' response to the high-dose per fraction of SBRT or SRS (6–8, 11–13). Indeed, it was reported that irradiation of experimental rodent tumors with 10 Gy or higher in a single dose induced severe vascular destruction (14–20), thereby causing indirect tumor cell death (19, 20). Other reports have also indicated that radiation-induced endothelial cell death and vascular dysfunction by high-dose irradiation induced secondary cell death in various types of tumors (21–25). It is of note that all these previous observations were made before SBRT and SBR became routine clinical practice for the treatment of human cancers. In the present study, we investigated in detail the kinetics of secondary cell death caused by 10- to 30-Gy irradiation in a single fraction, using FSaII fibrosarcomas of C3H mice. We also studied the effect of high-dose irradiation on the intratumor microenvironment to shed light on the mechanisms responsible for indirect cell death after high—dose-per-fraction irradiation.

Methods and Materials

Tumors and mice

Early generation FSaII tumor cells stored in liquid nitrogen were thawed and cultured in RPMI 1640 medium supplemented with 10% calf serum and antibiotics in an incubator in 5% CO_2 atmosphere at 37°C. Exponentially growing cells in culture were dispersed with 0.5% trypsin and washed, and approximately 2×10^5 viable tumor cells able to exclude trypan blue were injected subcutaneously into the right rear limbs of 5- to 6-week-old male C3H mice (26). All experiments were performed following a protocol approved by University of Minnesota Institutional Animal Care and Use Committee (Protocol number 0112A13064).

Irradiation of tumors and determination of cell survival

After the tumors grew to 6 to 7 mm in diameter, host mice were lightly anesthetized with a mixture of xylazine (20 mg/kg) and ketamine (100 mg/kg) in 0.1 ml of saline, and tumors were irradiated with 10, 15, 20, or 30 Gy of X rays in a single dose, using an X-Rad 320 Biological Irradiator (Precision X-Ray Inc). Irradiation parameters were 320 kVp, 12.5 mA, and 2-mm Al filter at a dose rate of 1.5 Gy/min. The x-ray machine was calibrated according to the procedures described in a recent report (27). Immediately after or 2, 3, and 5 days after irradiation, host mice were euthanized in a CO_2 chamber. Tumors were carefully excised, blotted, weighed, and minced with surgical scissors. Tumor pieces were then dispersed to single cells with mechanical and enzymatic means, using a tumor dissociation kit (Miltenyi Biotec). Resultant single-cell suspensions were passed through a sterile cell strainer (100 μm nylon mesh; Fisher Scientific). The total number of cells able to exclude trypan blue was counted for each tumor, and appropriate numbers of cells were plated onto T-75 cm^2 plastic culture flasks with 10 ml of RPMI 1640 medium supplemented with 10% calf serum and antibiotics. For each tumor, 3 different concentrations of cells were plated with 3 replicate cultures for each cell concentration (9 cultures per tumor). After incubation in a 5% CO_2 incubator for 9 to 10 days, the resultant colonies were fixed with 95% ethanol and stained with 1% crystal violet, and colonies containing >50 cells were counted. From the total number of cells harvested from each tumor and the plating efficiency of the cells, the total number of clonogenic cells in each tumor was calculated (19).

Immunohistochemical assessment of intratumor environment

Hypoxia and blood perfusion—At various times after tumors were exposed to 20 Gy in a single fraction, 75 mg/kg pimonidazole in 0.1 ml of saline was injected intraperitoneally (28). At 1 hour after the pimonidazole injection, 2 mg/kg Hoechst 33342 dye in 0.05 ml of saline was injected in the tail vein, and the animals were sacrificed 2 minutes later. Tumors were excised, quickly frozen, and processed for immunohistochemical study. After tissue samples were sectioned using a cryostat at 5-μm thickness, hypoxic cells in the tissue were detected with antipimonidazole antibody (mouse fluorescein isothiocyanate-monoclonal antibody diluted 1:50; Hypoxyprobe, Inc). Tumor blood vessels were marked with primary antibody against CD31 (rat anti-CD31, 1:100 dilution, BD Pharmingen) and a secondary antibody, anti-rat Alexa 647 (1:100 dilution) and then mounted in Vectashield mounting medium with 4, 6-diamidino-2-phenylindole dihydrochloride (DAPI; Vector Labs, Inc). Imaging of the hypoxic areas indicated by green pimonidazole fluorescence and perfused blood vessels filled with blue Hochest 33342 fluorescence dye was performed using an IX71 model fluorescence microscope workstation (Olympus) or a Scanscope FL (Aperio). Signals for the 2 indices in control and irradiated tumors were quantified using ImageJ software as described previously (28).

CA9, HIF-1α, VEGF, and endothelial cell detection in FFPE tissues—At various times after exposing tumors to 20 Gy in a single fraction, tumors were excised, fixed, and paraffin embedded. Subsequently, sections for histology were prepared: tissue was deparaffinized, boiled in 0.1 M citrate buffer (pH 6.0) for 30 min, and then incubated with 0.3% (v/v) hydrogen peroxide in methanol for 15 minutes. Sections were blocked with normal horse serum at room temperature for 30 min and immunostained overnight at 4°C

with primary antibodies against HIF1-α (1:100 dilution; code sc-53546; Santa Cruz Biotechnology), VEGF (1:100 dilution; code sc-1836, Santa Cruz Biotechnology), CD31 (1:100 dilution; code sc-1506, Santa Cruz Biotechnology), and carbonic anhydrase-9 (CA9; 1:1000 dilution; product NB100-417, Novus Biologicals, Littleton, CO). Target proteins were visualized using avidin-conjugated horseradish peroxidase with diaminobenzidine as substrate (Vector Laboratories) and counterstained with hematoxylin (29). Images for were obtained using a camera fitted to a Zeiss microscope.

Statistics

Statistical significance was determined with 2-tailed *t* test, nonparametric (Mann-Whitney) using Prism version 6.02 software (Graph Pad). Differences with a *P* value of <.05 were considered statistically significant.

Results

Cell death

The clonogenic cell number in each irradiated tumor was normalized as a fraction of the mean of the clonogenic cell numbers in 15 control tumors as shown in Figure 1A. In the tumors irradiated with 10 Gy in a single dose, surviving cell fractions determined after leaving the tumors in situ for 2 to 5 days were similar to that determined immediately after irradiation. After irradiation with 15 Gy (Fig. 1Ab), cell survival progressively decreased for 3 days. Delayed cell death after 20-Gy irradiation (Fig. 1Ac) was even more pronounced than that after 15-Gy irradiation. Although there was a slight increase in cell survival after the nadir in cell survival at days 2 and 3 after 15- or 20-Gy irradiation, cell survival in some individual tumors on day 5 after the irradiation was almost 2 logs less than that immediately after irradiation. After irradiation with 30 Gy (Fig. 1Ad), secondary cell death steadily progressed for 5 days after irradiation. Cell survival in some tumors on day 5 after 30-Gy irradiation was as much as 3 logs less than the mean cell survival immediately after 30-Gy irradiation. Cell survival at different times after irradiation shown in Figure 1A are summarized in columnar form in Figure 1B, for clarity. Cell survival 2 to 5 days after 15- and 20-Gy irradiation was significantly less than that immediately after irradiation ($P<.05$ and $P<.001$, respectively). After irradiation with 30 Gy, cell survival on the fifth day was also markedly less than that immediately after irradiation ($P<.001$).

Figure 2 shows the radiation cell survival curves based on cell survival determined immediately (day 0) or 5 days (day 5) after 10- to 30-Gy irradiation. Mean cell survival levels for each radiation dose are shown in Figure 1. Because of dose-dependent secondary cell death during 5 days after irradiation, the day 5 radiation survival curve was much steeper than the day 0 survival curve.

Intratumor microenvironment

Figure 3A shows that in the control tumors, most of the CD31-labeled blood vessels were associated with functional perfusion (Hoechst 33342 blue fluorescence), although some of the blood vessels in the hypoxic areas (green fluorescence) were weakly stained with Hoechst 33342 dye. In the tumors excised 2 days after 20-Gy irradiation, many of the CD31-

positive blood vessels were devoid of Hoechst 33342 dye, indicating that the vessels were static. Interestingly, as shown in Figure 3B, whereas 20-Gy irradiation markedly reduced the frequency of perfused vessels filled with Hoechst 33342 dye ($P<.015$), it did not significantly increase pimonidazole staining ($P<.2$).

Figure 4A shows that the level of CA9, which is one of the HIF-1α target genes and, thus, a cellular hypoxic marker, increased after 20-Gy irradiation. The increase in CA9 could be detected on the first day after irradiation, and the increase was significant on day 5 ($P<.05$), suggesting that 20-Gy irradiation increased tumor hypoxia. Levels of HIF-1α (Fig. 4B) significantly increased 1 to 3 days after 20-Gy irradiation ($P<.05$) and then slightly declined on day 5. VEGF expression (Fig. 4C) significantly increased on day 1 after 20-Gy irradiation and remained increased until 5 days after irradiation ($P<.05$). The frequency of CD31-stained microvessels (microvessel density) (Fig. 4D) increased slightly on days 1 to 3 and significantly on day 5 after 20-Gy irradiation ($P<.05$).

Discussion

In the present study using FSaII tumors of C3H mice, irradiation with 15-Gy or higher doses caused secondary cell death in a dose-dependent manner in addition to directly killing tumor cells (Figs. 1 and 2). Such secondary cell deaths after an exposure to high-dose radiation appeared to be due mainly to vascular occlusion and ensuring increase in hypoxia.

SBRT with 30 to 60 Gy in 2 to 5 fractions has been demonstrated to be highly effective for controlling various human tumors (1, 2). Likewise, SRS of cranial lesions and extracranial tumors with 15 to 25 Gy in a single dose has been shown to result in very high rates of local control (3–5). The number of viable tumor cells in 1 g of tumors has been estimated to be approximately 10^8 to 10^9 (30), implying that 8 to 9 logs of tumor cells must be sterilized for the control of 1 g of tumors. If it is assumed that SBRT and SRS kill tumor cells only through DNA double-strand breaks and that 10% to 20% of tumor cells are hypoxic cells, SBRT or SRS with the doses currently used would reduce the viable tumor cell numbers by only 3 to 6 logs (31, 32). It is then apparent that SBRT and SRS are highly effective because they kill significant fractions of tumor cells through other mechanisms in addition to directly killing tumor cells by DNA double-strand breaks.

In the present study with FSaII tumors, the extent of cell death determined at 2 to 5 days after 10-Gy irradiation was similar to that immediately after irradiation (Fig. 1A and 1B). On the other hand, the surviving cell fractions at 2 to 3 days after irradiation with 15 or 20 Gy in a single dose were markedly less than that immediately after irradiation, demonstrating that secondary cell death occurred in significant amounts 2 to 3 days after irradiation. The means of surviving cell fractions on the fifth day after 15- or 20-Gy irradiation were slightly higher than those on the second or third day, probably due to repopulation of tumor cells, although cell survival in some individual tumors remained markedly low. After cells underwent irradiation with 30 Gy, secondary cell death progressed continually for 5 days, the limit of the present study (Fig. 1Ad). It is of note that the surviving cell fraction in some tumors 5 days after 30-Gy irradiation was as low as 10^{-6}. Figure 2 shows that the radiation survival curve obtained 5 days after irradiation was much

steeper than that determined immediately after irradiation. This downward shift of the slope of radiation survival curve was apparently due to death of hypoxic cells in a radiation dose-dependent manner during 5 days after irradiation. This observation clearly demonstrated that the radiation resistance conferred by hypoxia may be substantially diminished in tumors treated with SBRT and SRS.

A recent review of radiation-induced vascular changes in tumors concluded that irradiation of tumors with 5 to 10 Gy in a single dose causes relatively mild vascular damage, whereas increasing the radiation dose to higher than 10 Gy per fraction induces severe vascular destruction (12). In the present study with FSaII tumors of mice, the frequency of blood vessels perfused with Hoechst 33342 dye was significantly reduced at 2 days after 20-Gy irradiation (Fig. 3), demonstrating that tumor blood vessels were severely occluded. Importantly, many CD31-positive blood vessels in the irradiated tumors were devoid of Hoechst 33342 dye, demonstrating that the endothelial cells were still viable but the blood vessels were static. As shown in Figure 4, levels of CA9, a marker for hypoxic cells, and HIF-1α significantly increased as early as 1 day after 20-Gy irradiation, clearly suggesting that the intratumor microenvironment was hypoxic as a result of the vascular damage. Interestingly, the levels of pimonidazole labeling remained essentially unchanged for 2 days after 20-Gy irradiation (Fig. 3) despite the significant increase in CA9 and HIF-1α expression, (Fig. 4). This may seem contradictory, but it appeared that the intraperitoneally injected pimonidazole was unable to reach the hypoxic regions in which blood vessels were severely occluded. The lack of increase in pimonidazole labeling may also be due to a decline in the population of viable tumor cells able to induce reduction of pimonidazole. Interestingly, the number of blood vessels labeled with CD31 actually increased 5 days after 20-Gy irradiation (Fig. 4D). This may be attributed to a condensation of vasculature and endothelial cells, which are damaged and yet CD31-positive as a consequence of the lysis of dead tumor cells (18). Taken together, we may conclude that the delayed secondary tumor cell death in FSaII tumors after irradiation with 15 to 30 Gy in the present study resulted from the general deterioration of intratumor microenvironment ensuing from vascular obstruction.

Major outstanding variables in treating tumors with SBRT or SRS are the approximate optimal fraction size, the number of fractions, and the total dose. In a previous study with Walker tumors of rat (19), 10-Gy irradiation caused a secondary cell death. On the other hand, in the present study with FSaII tumors, 10-Gy irradiation induced virtually no secondary cell death, whereas 15-Gy irradiation caused marked secondary cell death (Fig. 1). These results indicated the existence of a critical radiation dose for induction of secondary cell death, which may vary depending on tumor type, site of tumor growth, and type of host. The efficacy of repeated irradiation with doses lower than the critical dose to induce secondary cell death remains to be elucidated, given that fractionated SBRT and SRS with relatively low doses per fraction are often used.

It has been suggested that the high efficacy of SBRT and SRS is due to their ability to stimulate antitumor immunity (33–35). However, it is unlikely that the massive secondary cell death which occurs within 2 to 3 days after an exposure to high-dose irradiation is caused by elevation of antitumor immune response, because a significant increase in tumor-

specific immune systems as a result of high-dose irradiation of tumors takes longer than at least 1 week (34). Moreover, 20-Gy irradiation in a single dose effectively caused secondary cell death in 2 to 3 days, even in HT-1080 human sarcoma xenografts grown in nude mice, whose immune system is compromised (7). This conclusion, however, does not exclude the possibility that strong antitumor immunity may be evoked across days to weeks after high-dose-per-fraction irradiation as a consequence of the release of a larger amount of tumor antigens from the dying or dead tumor and stromal cells.

In contrast to our conclusions that indirect cell death is involved in the response of tumors to SBRT and SRS, it has been reported that radiobiological principles of conventional fractionated radiation therapy are sufficient to account for the high clinical efficacy of SBRT and SRS (9, 10). This controversy highlights the need for further detailed investigations to shed light on the biological mechanisms of SBRT and SRS.

Conclusions

In FSaII tumors of C3H mice, irradiation with 15 to 30 Gy in a single dose caused dose-dependent secondary cell death, most likely by deteriorating intratumor microenvironment by vascular damage. Whether similar indirect cell death due to vascular damage plays a role in the response of human tumors to ablative SBRT or SRS remains to be investigated.

Acknowledgments

This study was supported by grants from Minnesota Foundation and Elekta, by US National Institutes of Health/National Cancer Institute grant CA44114, and Nuclear Research and Development Program grant NRF 2013M2A2A7043580 from the National Research Foundation of Korea, funded by Ministry of Science, ICT, and Future Planning.

We thank Dr Seymour H. Levitt for his interest and encouragement in the present work.

References

1. Nagata Y. Stereotactic body radiation therapy for early stage lung cancer. Cancer Res Treat. 2013; 45:155–161. [PubMed: 24155673]
2. Timmerman R, Paulus R, Galvin J, et al. Stereo-tactic body radio-therapy to treat medically inoperable early stage lung cancer patients. J Am Med Assoc. 2010; 303:1070–1076.
3. Cho, LC.; Fonteyne, V.; DeNeve, W.; Lo, SS.; Timmerman, RD. Stereotactic body radiotherapy. In: Levitt, SH., et al., editors. Technical Basis of Radiation Therapy: Practical Clinical Application. New York: Springer Publishing Co; 2012. p. 363-400.
4. Sperduto PW. A Review of stereotactic radiosurgery in the management of brain metastases. Technol Cancer Res Treat. 2003; 2:105–110. [PubMed: 12680790]
5. Staehler M, Bader M, Cascuscelli J, et al. Single-fraction radiosurgery for the treatment of renal tumors. J Urol. 2015; 193:771–775. [PubMed: 25132240]
6. Song CW, Cho LC, Yuan J, et al. Radiobiology of stereotactic body radiation therapy/stereotactic radiosurgery and the linear-quadratic mode. Int J Radiat Oncol Biol Phys. 2013; 87:18–19. [PubMed: 23608235]
7. Song CW, Park I, Cho LC, et al. Is there indirect cell death involved in response of tumor to SRS and SBRT? Int J Radiat Oncol Biol Phys. 2014; 89:924–925. [PubMed: 24969800]
8. Sperduto PW, Song CW, Kirkpatrick J, et al. A hypothesis on indirect cell death in the radiosurgery era. Int J Radiat Oncol Biol Phys. 2015; 91:11–13. [PubMed: 25835617]

9. Brown JM, Brenner DJ, Carlson DJ. Dose escalation, not “new biology” can account for the efficacy of stereotactic body radiation therapy with non-small cell lung cancer. Int J Radiat Oncol Biol Phys. 2013; 85:1159–1160. [PubMed: 23517805]
10. Brown JM, Carlson DJ, Brenner DJ. The tumor radiobiology of SRS and SBRT: Are more than the 5Rs involved? Int J Radiat Oncol Biol Phys. 2014; 88:254–262. [PubMed: 24411596]
11. Song, CW.; Park, HJ.; Griffin, RJ.; Levitt, SH. Radiobiology of stereotactic radiosurgery and stereotactic body radiation therapy. In: Levitt, SH., et al., editors. Technical Basis of Radiation Therapy: Practical Clinical Application. New York: Springer Publishing Co; 2012. p. 51-61.
12. Park HJ, Griffin RJ, Hui S, et al. Radiation-induced vascular damage in tumors: Implications of vascular damage in ablative hypofractionated radiotherapy (SBRT and SRS). Radiat Res. 2012; 177:311–327. [PubMed: 22229487]
13. Song CW, Kim MS, Cho LC, et al. Radiobiological basis of SBRT and SRS. Int J Clin Oncol. 2014; 19:570–578. [PubMed: 24993673]
14. Song CW, Levitt SH. Effect of X irradiation on vascularity of normal tissues and experimental tumor. Radiology. 1970; 94:445–447. [PubMed: 5412822]
15. Song CW, Levitt SH. Vascular changes in Walker 256 carcinoma of rats following X irradiation. Radiology. 1971; 100:397–407. [PubMed: 5147407]
16. Song CW, Payne T, Levitt SH. Vascularity and blood flow in X-irradiated Walker carcinoma 256 of rats. Radiology. 1972; 104:693–697. [PubMed: 5051488]
17. Wong HH, Song CW, Levitt SH. Early changes in the functional vasculature of Walker carcinoma 256 following irradiation. Radiology. 1973; 108:429–434. [PubMed: 4719050]
18. Song CW, Sung JH, Clement JJ, et al. Vascular changes in neuroblastoma of mice following X-irradiation. Cancer Res. 1974; 34:2344–2350. [PubMed: 4843534]
19. Clement JJ, Tanaka N, Song CW. Tumor reoxygenation and post-irradiation vascular changes. Radiology. 1978; 127:799–803. [PubMed: 663181]
20. Clement JJ, Song CW, Levitt SH. Changes in functional vascularity and cell number following X-irradiation of a murine carcinoma. Int J Radiat Oncol Biol Phys. 1976; 1:671–678. [PubMed: 977401]
21. Garcia-Barrps M, Paris F, Cordon-Cardo C, et al. Tumor response to radiotherapy regulated by endothelial cell apoptosis. Science. 2003; 3000:1155–1159.
22. Cramer, W. Tenth Scientic Report. Imperial Cancer Research Fund; London: 1932. Experimental Observation on the therapeutic action of radium; p. 95-123.
23. Lasnitzki I. Quantitative analysis of the direct and indirect action of X radiation on malignant cells. Br J Radiol. 1947; 20:240–247. [PubMed: 20243691]
24. Szeifert G, Massager N, DeVriendt D, et al. Observation of intracranial neoplasm treated with gamma knife radiosurgery. Neuosurg. 2002; 5(suppl):623–626.
25. Denekamp J. Vascular endothelium as the vulnerable element in tumours. Acta Radiol Oncol. 1984; 23:217–225. [PubMed: 6208746]
26. Griffin RJ, Okajima K, Ogawa A, et al. Radiosensitization of two murine tumours with mild temperature hyperthermia and carbogen breathing. Int J Radiat Oncol Biol Phys. 1999; 75:1299–1306.
27. Azim R, Alaei P, Spezi E, et al. Characterization of an orthovoltage biological irradiator used for radiobiological research. J Radiat Res. 2015; 56:485–492. [PubMed: 25694476]
28. Dings RP, Loren M, Heum H, et al. Scheduling of radiation with angiogenesis inhibitors anginex and Vastin improves therapeutic outcome via vessel normalization. Clin Cancer Res. 2007; 1:3395–3402. [PubMed: 17545548]
29. Cao D, Hou M, Guan YS, et al. Expression of HIF-1alpha and VEGF in colorectal cancer: Association with clinical outcomes and prognostic implications. BMC Cancer. 2009; 9:432. [PubMed: 20003271]
30. Monte UD. Does the cell number 109 still really fit one gram of tumor tissue? Cell Cycle. 2009; 8:505–506. [PubMed: 19176997]

31. Leith JT, Cook S, Choughle P, et al. Intrinsic and extrinsic characteristics of human tumors relevant to radiosurgery: Comparative cellular radiosensitivity and hypoxic percentages. Acta Neurochir Suppl. 1994; 62:18–27. [PubMed: 7717130]

32. Fowler JF, Wolfgang AT, Fenwick JD, et al. A challenge to traditional radiation oncology. Int J Radiat Oncol Biol Phys. 2004; 60:1241–1256. [PubMed: 15519797]

33. McBride, WH.; Schaue, D. In situ tumor ablation with radiation therapy: Its effect on the tumor microenvironment and anti-tumor immunity. In: Keisari, Y., editor. Tumor Ablation. New York: Spinger Publishing Co; 2012. p. 109-119.

34. Lee Y, Auh SL, Wang Y, et al. Therapeutic effects of ablative radiation on local tumor require CD8 T cells: Changing strategies for cancer treatment. Blood. 2009; 114:589–595. [PubMed: 19349616]

35. Matsumura S, Wang B, Kawashima N, et al. Radiation induced CXCL16 release by breast cancer cells attracts effector T cells. J Immunol. 2008; 181:3009–3107. [PubMed: 18713971]

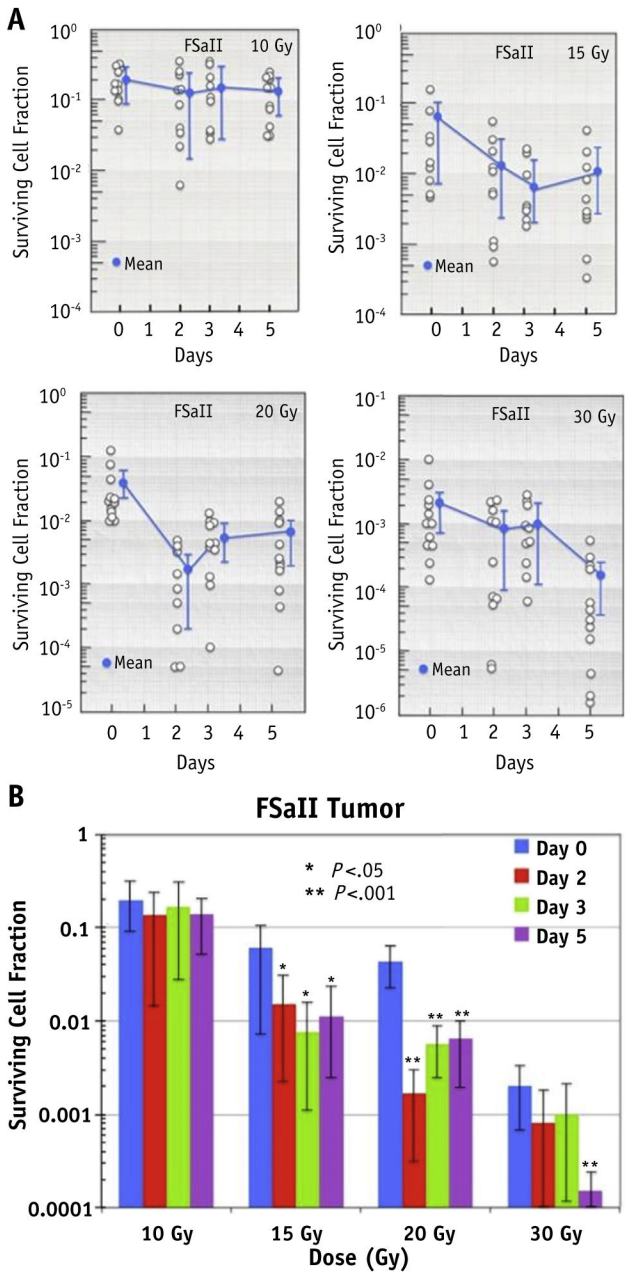

Fig. 1.

(A) Effects of irradiation on the cell survival in FSaII tumors grown subcutaneously in the hind limb of C3H mice. Cell survival was determined using in vivo—in vitro excision method, and cell survival in irradiated groups was normalized to that in the unirradiated control tumors. Open circles are surviving cell fraction in individual tumors, and closed circles are the means of surviving cell fractions in each group consisting of 9 to 12 tumors. Bars indicate SD. (B) Surviving cell fractions shown in A are summarized in columns for clearer comparisons. Mean ± SD surviving fractions of 9 to 12 tumors immediately and at 2, 3, and 5 days after 10- to 30-Gy irradiation are shown. Statistically significant differences

among the cell survival immediately after irradiation (Day 0) and that 2, 3 or 5 days after irradiation are indicated with *P<.05 and **P<.001.

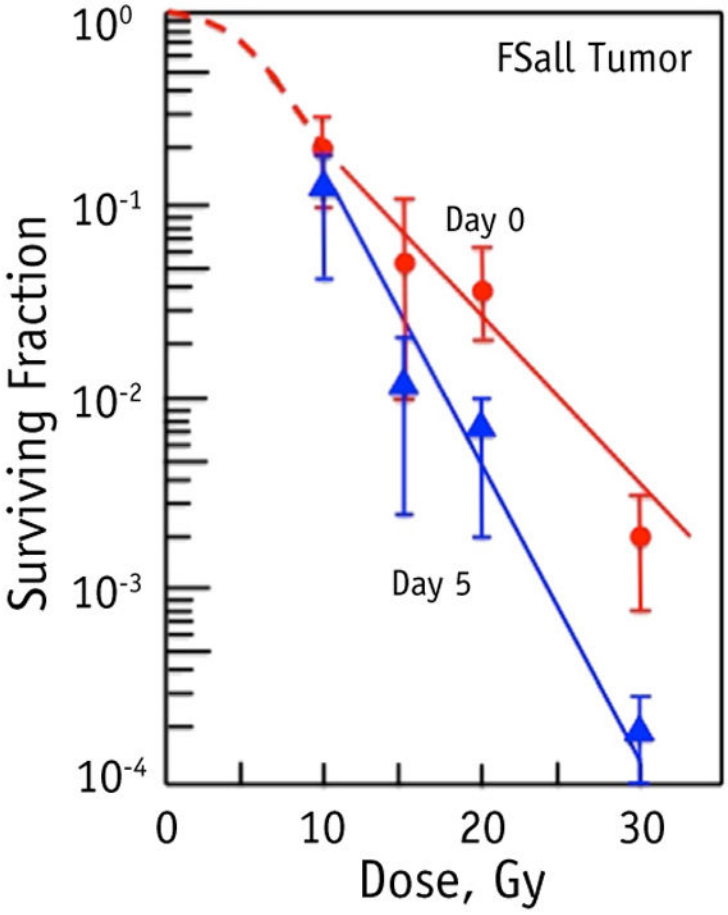

Fig. 2.

Radiation survival curves of tumor cells in vivo obtained immediately (Day 0) and at 5 days (Day 5) after irradiation. Data are means ± SD from A.

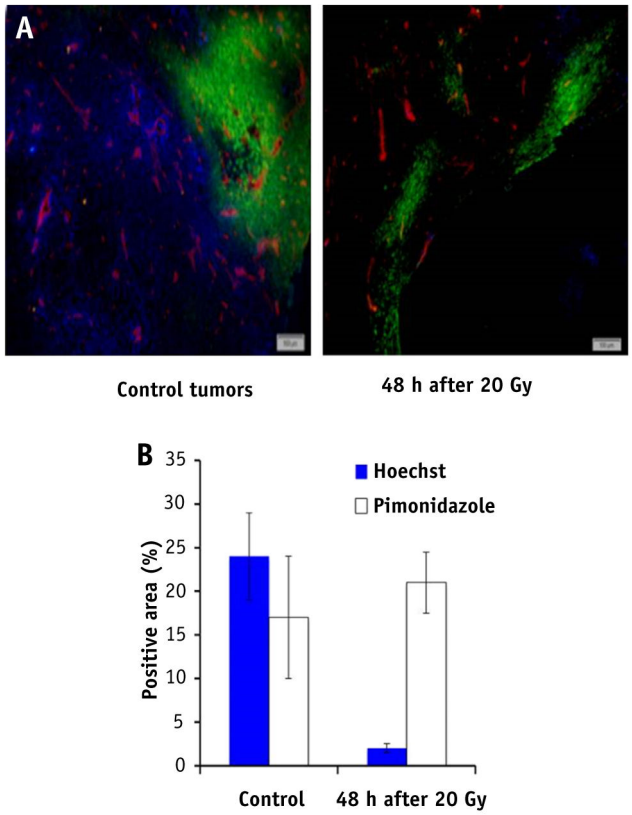

Fig. 3.

(A) Immunohistological images of hypoxia, blood perfusion, and blood vessels. Representative sections from a control tumor and a tumor excised 48 hours after irradiation with 20 Gy are shown. Blood vessels (endothelial cells) are indicated with CD31 marker (red); hypoxic areas are labeled with pimonidazole (green); and blood perfusion is indicated by Hoechst 33342 (blue). (B) Areas positive for Hoechst 33342 (perfusion) and pimonidazole (hypoxia) in tissue sections were quantified using Image J software. Hypoxic areas (green) are shown as a percentage of total area in each section. Five sections from each of 4 tumors were analyzed, and means ± SEM are shown. Hypoxia signals between the control and the irradiated tumors was not significantly different ($P<.2$), whereas differences between perfusion in control and that in irradiated tumors were significant, with $P<.015$.

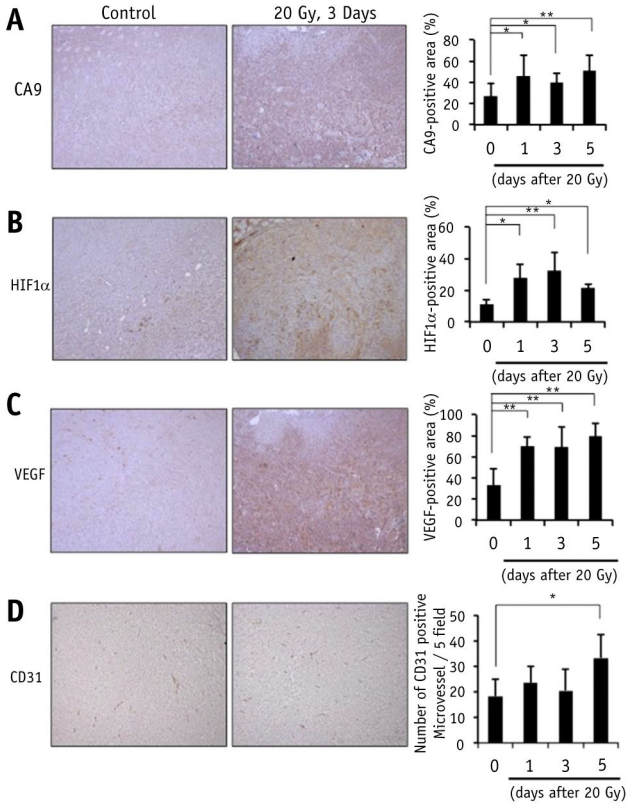

Fig. 4.

Immunohistological images of CA9, HIF-1α, VEGF, and CD31. Representative sections from control tumors and tumors excised 3 days after 20-Gy irradiation are shown. (A) Brown stain = hypoxia marker CA9 (carbonic anhydrase 9). (B) Brown stain = HIF-1α. (C) Reddish brown stain = VEGF. (D) dark brown = CD31-labled microvessels. Five sections from each of 4 tumors (20 sections) were examined, and means ± SD percentage of the positive area are shown in the bar graphs for CA9, HIF-1, and VEGF. The bar graph for CD31 shows the average number of CD31-labeled microvessels in 5 sections. Statistically significant differences between the control and the irradiated groups are indicated with **P*<. 1 and ***P*<.05.